Simultaneous morphological and functional imaging of the honeybee's brain by two-photon microscopy

A. Haase([1])(*), E. Rigosi([2])([3]), G. Anfora([2]), G. Vallortigara([3]), C. Vinegoni([4]), and R. Antolini([1])

([1]) *Physics Department, University of Trento, Via Sommarive 14, 38050 Povo, Italy*
([2]) *IASMA Research and Innovation Center, Fondazione E. Mach, via E. Mach 1, 38010 San Michele all'Adige, Italy*
([3]) *Center for Mind/Brain Sciences, University of Trento, Corso Bettini 31, 38068 Rovereto, Italy*
([4]) *Center for Systems Biology, Massachusetts General Hospital, Harvard Medical School, 185 Cambridge Street, Boston, Massachusetts 02114, USA*

Summary. — Thanks to its rather simply structured but highly performing brain, the honeybee (*Apis mellifera*) is an important model for neurobiological studies. Therefore there is a great need for new functional imaging modalities. Herein we report on the development and new findings of a platform for in-vivo functional and morphological imaging of the honeybee's brain, focusing on its primary olfactory centres, the antennal lobes (ALs). The experimental setup consists of a two-photon microscope combined with a synchronized odour stimulus generator. Our imaging platform allows for simultaneously obtaining both morphological measurements of the AL's functional units, the glomeruli, and in-vivo calcium recording of their neural activities. We were able to record the characteristic glomerular odour response maps to odour stimuli applied to the bee's antennae. Our approach has offers several advantages over the commonly used conventional fluorescence microscopy. Two photon microscopy provides substantial enhancement in both spatial and temporal resolutions, while minimizing photo-damage. Calcium recordings show a four-fold improvement in the functional signal with respect to the techniques available up to now. Finally, the extended penetration depth, thanks to the infrared excitation, allows for functional imaging of profound glomeruli which have not been optically accessible up to now.

PACS 87.19.lt – Sensory systems: visual, auditory, tactile, taste, and olfaction.
PACS 87.19.lh – Optical imaging of neuronal activity.
PACS 87.64.mn – Multiphoton.

(*) albrecht.haase@unitn.it

1. – Introduction

Many of the important advances in neuroscience have been linked to the development of new investigative tools. The action potentials of single neurons have been measured for the first time by intracellular recording [1]. A next important step was the development of a new class of voltage-sensitive dyes [2] which offered the possibility to optically image the functionality of neuronal circuits at the level of single neurons as well as the whole brain. In recent years the development of calcium-sensitive dyes [3] had an incredible impact on functional neuroimaging, providing a universal and sensitive method to study distinct information processing pathways in whole neural networks. A further improvement was brought by two-photon laser scanning microscopy [4], which via calcium recording allowed for in-vivo real-time monitoring of complex neural circuits down to several hundred micrometers within the specimen [5].

This paper presents our efforts in developing two-photon calcium imaging of the honeybee brain. With less than one million neurons, the honeybee is an excellent model for the study of neural systems of intermediate complexity [6], and the brain's dimensions of approximately 2.5mm x 1.6mm x 0.8mm [7] make it an ideal candidate for two-photon microscopy [8]. In the past years several different optical imaging approaches have allowed to gain tremendous insights into the bee's olfactory system. Along the antennae $\sim$60000 olfactory receptor neurons (ORNs) send their axons to the primary processing centres in the brain, the antennal lobes (ALs). These consist of 160 functional units, synaptic centre called glomeruli, each of them connected to one odour receptor family only. The glomeruli interact via $\sim$4000 local interneurons. The AL can be subdivided into 4 regions named T1-T4 [9], with a fundamental difference in how they relay via the $\sim$950 projection neurons (PNs) to the higher brain centres. Class T1 projects along the lateral antenno-cerebralis tract (l-ACT) first into the lateral horn (LH) and than into the mushroom body (MB), while the other classes T2-T4 project along the median antenno-cerebralis tract (m-ACT) first into the MB and than into the LH [10] .

Early pioneering efforts in functional imaging of this system using voltage-sensitive dyes [11] have paved the way for a series of extremely successful experiments using optical fluorescence microscopy and various staining techniques to investigate different aspects of the odour processing network. A first breakthrough in the systematic description of the odour coding in the AL was achieved by using calcium-sensitive cell-permeant dyes which allowed visualizing the activity patterns of a big part of the T1 glomeruli [12]. These signals were found to be dominated by the ORNs, the input channels to the AL. The method of selective backfill staining of specific neurons with membrane-impermeable dyes [13] has instead allowed to record the AL's output signal from the PNs [14].

Besides the functional imaging studies also the morphology of the olfactory centres has been investigated extensively [9], more recently by confocal microscopy [15, 7], and evidence of strong glomerular plasticity in the ALs has been reported lately [16]. While linear microscopy techniques have been proven over the last years to be very effective in characterizing basic principles of this complex neuronal system, their intrinsic limitations have become more and more obvious [17]. Full-field microscopy does not offer sufficient axial resolution to pinpoint the exact origin of functional signals from deeper glomeruli and lacks the temporal resolution to determine whether valuable information might be encoded in the temporal structure of the recorded odour-evoked signals. Whereas confocal microscopy due to its intrinsic photo-damaging properties poses severe time constraints to in-vivo imaging sessions and has therefore only be used for morphological studies of the dissected and embedded brain.

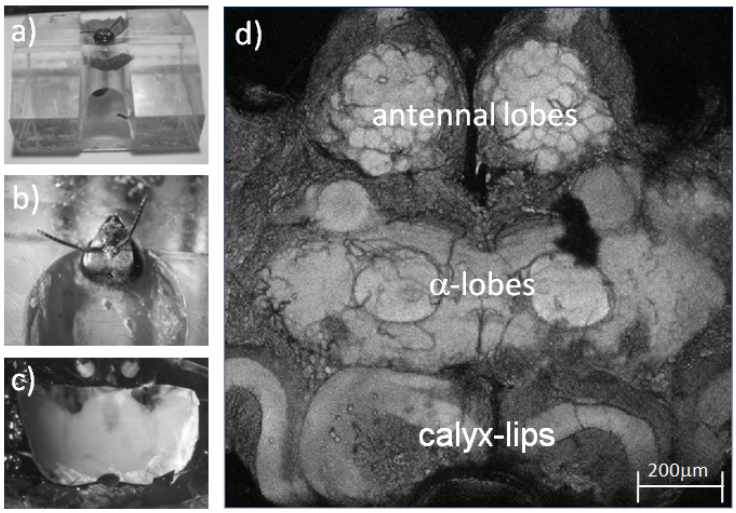

Fig. 1. – a,b) Bee attached to the imaging stage. c) Exposed brain, after the cuticula has been opened and glands and trachea have been removed. d) Morphological image of a big part of the honeybee brain, acquired with a 10x lens with a field of view of 1.2mm, after bath-staining with the membrane selective dye RH795 (Invitrogen). It allows for the identification of the antennal lobes and the mushroom body with its α-lobes and calyx-lips. These images help finding the correct injection position into the antenno-cerebralis tracts for antennal lobe backfill-staining.

In this paper we report on the development and new findings of a neural imaging platform for functional imaging of the honeybee's antennal lobe. Our system permits to overcome the imaging impediments currently faced by neuroscientists. It enables us to acquire both in-vivo functional and morphological data from the ALs. Functional data show that we have been able for the first time to longitudinally resolve active glomeruli, while the high temporal resolution permits a reconstruction of the neuron's firing rate [18]. Besides the well investigated T1 glomeruli, projecting into the l-ACT, the intrinsic two-photon optical penetration is deep enough to study also the other glomeruli classes T2 and T3 projecting into the m-ACT, which have not been optically accessible in the ALs yet. Electrophysiological studies [19, 20] and imaging of their axon terminals [21] have suggested distinctive functional differences with respect to the l-ACT glomeruli.

2. – Methods

Bees have been collected from outdoor hives and prepared in accordance to a well established protocol [22]. After chilling to immobility, bees were fixed to a custom made imaging stage [Fig. 1(a,b)] using dental waxes (Kerr; Siladent). Then a window was cut into the head's cuticula above antennal lobes and mushroom body, glands and trachea were gently moved aside [Fig. 1(c)], and a solution of calcium sensitive dye (fura2-dextran, Invitrogen) and 2% Bovine Serum Albumin (Sigma-Aldrich) was injected by dye-coated micro-tips into the antenno-cerebralis tracts below the α-lobe [Fig. 1(d)]. Finally, the cuticula was carefully closed and the animals were stored for 20h in a dark, cool, and humid place in order for the dye to diffuse into the AL. Before the imaging session, the cuticula, the glands, and the trachea above the AL were removed. A pond was formed

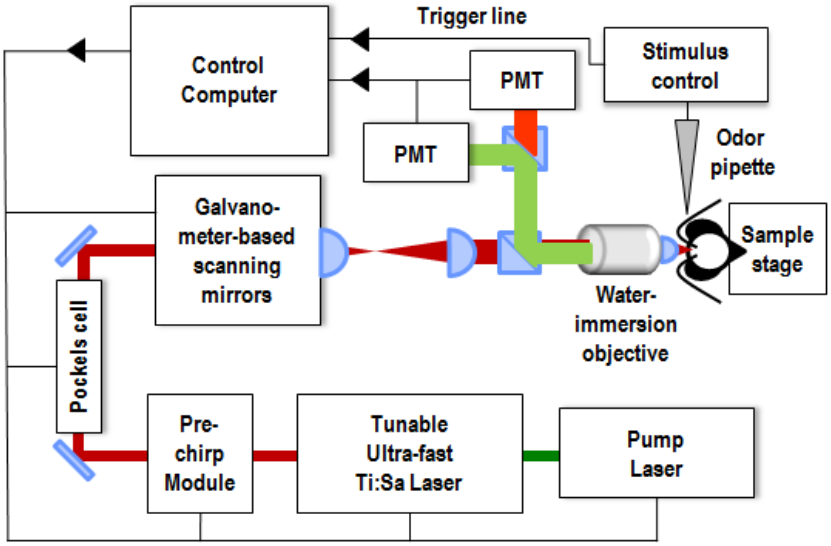

Fig. 2. – a) Experimental setup: A tunable ultra-fast pulsed laser serves as the light source. After pulse shaping in a pre-chirp module and intensity control by a Pockels cell, the beam is scanned by galvo-mirrors and focused by a water immersion objective to the exposed AL of a bee, fixed to a mounting stage. The fluorescence signal is collected in reflection, separated by way of a dichroic mirror and detected by photomultiplier tubes (PMT). A stimulus controller produces time-gated odour puffs which are synchronized with all command signals and acquisitions by a common gate.

above the imaging region using plastic plates, sealed with silicon (Kwik-Sil, WPI), and filled with specific Ringer's solution [22], imitating the brain's natural environment. The imaging setup is sketched in Figure 2. It consists of a two-photon microscope (Ultima IV, Prairie Technologies) combined with an ultra-short pulsed laser (Mai Tai Deep See HP, Spectra-Physics). The laser was tuned to 800nm for fura-2 excitation. The two-photon absorption is optimized by pulse re-shaping for dispersion compensation in a pre-chirp module. A Pockels cell controls the beam intensity and galvo-mirrors allow for fast and variable scanning. The beam is strongly focussed onto the sample by a water immersion objective (40x, NA 0.8, Olympus). Fluorescence is collected in reflection by the same objective, separated from the backscattered excitation light by a dichroic beam-splitter, filtered by a 70nm band-pass filter centred at around 525nm (both Chroma Technology), and detected by Photomultiplier tubes (Hamamatsu Photonics). A point-spread-function measurement verified the microscope's resolution to be diffraction limited to $\sigma_{x,y}$=230nm in the plane and $\sigma_z = 1.1\mu$m axially. Optimal signal-to-noise ratio was achieved with laser powers of about 10mW at the sample surface without observing any induced photo-damage during the measurement. The temperature of the experimental environment was stabilized to 29°C.

To allow for recordings with temporal resolution as high as 15ms, the excitation laser was scanned in an arbitrary horizontal plane along one-dimensional custom-defined traces [Fig. 3(a)]. These line scan traces where chosen to cross all glomeruli of interest [Fig. 3(b)]. All acquired data have been corrected for photo-bleaching, while 2D running-average filtering was used to reduce the noise level. Spatial averaging was performed

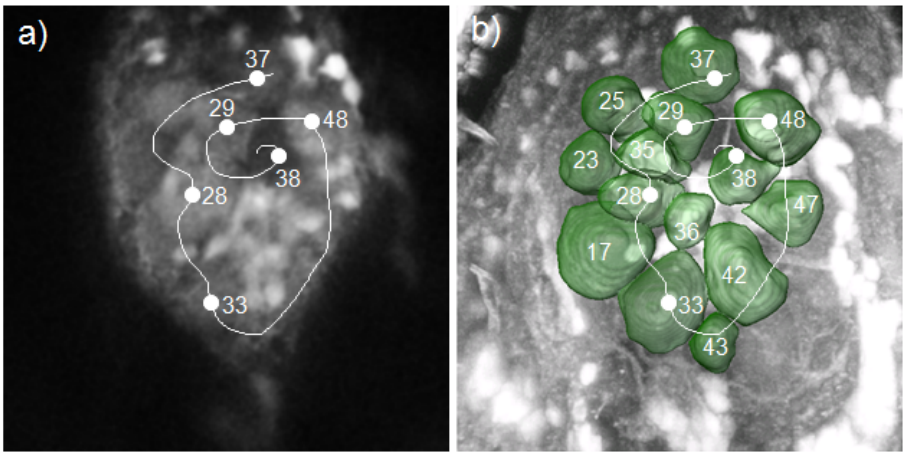

Fig. 3. – a) Image of a left antennal lobe at 25μm depth: The line indicates the laser scanning trace, the dots label the measurement's reference positions corresponding to the vertical lines in Figure 4. (b) Axial projection view of the AL volume image stack, superimposed by the reconstructed surface plots of the T1 glomeruli crossed by the scanning trace. The glomeruli are identified and labelled according to [15].

over a typical glomerulus size of 30μm, while temporal averaging was applied over 80ms preserving all main dynamic features of the data.

A stimulus controller (CS-55, Syntech) delivered odour stimuli to the bee's antennae without changing the total air flux to avoid mechanical stimuli. The odour puffs come from Pasteur pipettes in which 10μL of an odour solution (1:10 in mineral oil) were deposited on a piece of filter paper.

All command signals and acquisitions were controlled by a common gate which allows precise synchronization of the involved pulses. The experimental cycle began by starting the image acquisition. After 3s the stimulus generator received a trigger releasing an odour puff of 2s length. The exact arrival time of the odour at the bee antenna was measured and found to be stable within 10ms, which allows e.g. accurate measurements of the neuronal response delay. After 9s image acquisition stopped and automatic data evaluation started.

Response recordings are repeated three times the same stimulus with one minute recovery intervals in between. Averaging over these data sets is applied if only the total response strength is of interest. This serves to reduce random fluctuations and becomes especially useful at higher imaging depths.

Thanks to the reduced photo-damage characteristics of two-photon microscopy, due to the limited absorption volume in the sample, the imaging sessions could be extended up to 5 hours before we noticed an essential drop in the brain activity.

Data analysis was automatically executed during the experiments by Matlab (Mathworks) scripts. Later post-processing for 3D reconstruction, image segmentation, and volumetric measurements was performed using the software Amira (Visage Imaging).

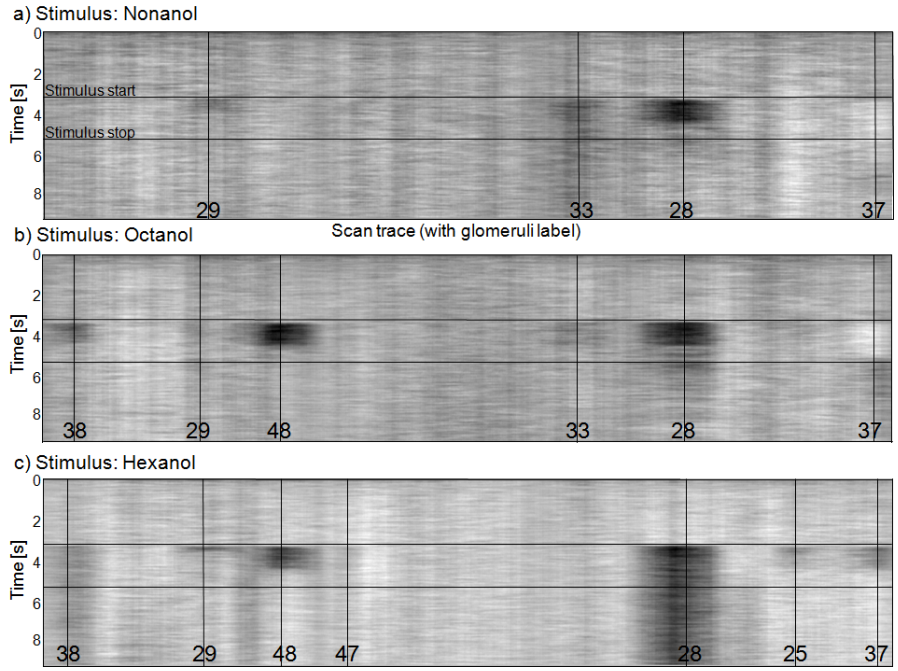

Fig. 4. – Calcium response maps for three different odour stimuli: (a) 1-Nonanol, (b) 1-Octanol, and (c) 1-Hexanol. Temporal changes along the scanning trace in Figure 3 are mapped. The x-axis shows the scan line, the y-axis time, the stimulus period after 3s is enclosed by the horizontal lines, responding glomeruli centres are marked by vertical lines, numbers label the identified T1 glomeruli according to [15].

3. – Results

In a first experiment, we recorded the spatio-temporal functional activity in the AL by measuring the two-photon calcium response signal along the line traces indicated in Figure 3. To compare the performance of our imaging setup with conventional methods, we used as odour stimuli three well studied floral components [23]: 1-Nonanol, 1-Octanol, and 1-Hexanol. Enhanced neural activity, leading to an increasing intra-neuronal calcium concentration, causes a drop in the measured two-photon fluorescence intensity, producing dark bands in the scanlines-over-time maps at the positions of the corresponding glomeruli. We detected response signals of up to 20% intensity change, which is more than 4 times higher than in comparable experiments using wide field imaging. The recorded odour response maps are shown in Figure 4 and reproduce features which have already been observed by conventional single-photon fluorescence microscopy, such as the very strong response of glomerulus T1-28 to all tested odours increasing with the odour's carbon chain length, and the somewhat weaker response of T1-33 decreasing with the odour's carbon chain length [24, 23]. Likewise, it has been found that 1-Hexanol produces the broadest response spectrum of the tested odours. Strikingly different from previously published data obtained with full-field microscopy [23] are the quite strong responses of glomeruli T1-48 to 1-Octanol and 1-Hexanol and the strong inhibitive response of T1-37 to 1-Nonanol and 1-Octanol, which might be due to the enhanced sensitivity of our

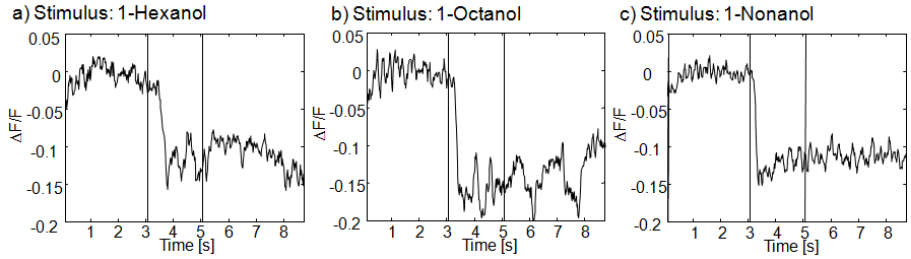

Fig. 5. – Single temporal response functions of the strongest responding glomerulus T1-33 in the maps of Figure 4, stimulated by 1-Hexanol in (a), 1-Octanol in (b), and 1-Nonanol in (c). The relative change in fluorescence is plotted as a function of time, the stimulus period after 3s is enclosed by vertical lines.

imaging system.

The high temporal resolution is demonstrated in Figure 5. Single response curves of glomerulus T1-33 to all three tested odours are depicted. Interesting features are a response delay which varies with the odour stimuli, and oscillatory features which might also contain odour coding information. The temporal resolution and the precise synchronization allow to analyze these potential temporal components of the olfactory code systematically. Both response latency [19] as well as synchronized oscillations [25] previously observed in electrophysiological measurements are hypothesized to be part of a general odour code.

Finally, we have exploited the larger penetration depth and the higher axial resolution offered by our setup. In Figure 6(a) we present an morphological images from a stack down to 270μm, representing the glomerular regions within the AL. We restrict the volumetric reconstruction of the single glomeruli to a depth of $\approx$200μm, down to which we were so far able to identify glomeruli with certainty. Figure 6(b) shows a projection view along the anterior-posterior axis (above) together with a surface plot of the identified glomeruli (below). Figure 6(c) shows a projection view along the dorso-ventral axis together with the identified glomeruli. This shows the depth limit for obtaining morphological information is $\approx$400μm. The reconstructed glomeruli have the following color code: green ones belong to the T1 sensory group projecting into the l-ACT axonal tract, while blue and red coloured ones belong to the deeper laying T2 and T3 groups, respectively, both projecting into the m-ACT. Apart from a few exceptions, the T2 and T3 glomeruli have never been optically accessible in-vivo because of their position below the surface or below the penetration depth limit of conventional microscopy.

The maximum penetration depth for clear functional imaging was found to be 150μm. Figure 7 shows odour response maps to a 1-Hexanol stimulus at different depths within the AL. The high axial resolution shows strongly changing response pattern at the different depths, due to the contribution of different glomeruli. The identified glomeruli are marked and labelled according to [15]. The green coloured points represent signals from the T1 tract. In some of the cases the glomeruli are located in an upper layer above the imaging plane and the signal comes only from the few projection neurons connected to them. In these cases the absolute fluorescence signal is very faint, but never the less a relative drop of up to 20% can be detected also here. The data points coloured in blue and red mark glomeruli from the T2 and T3 tract, respectively. These glomeruli are located in the focal plane leading to a strong absolute fluorescence signal. For the first

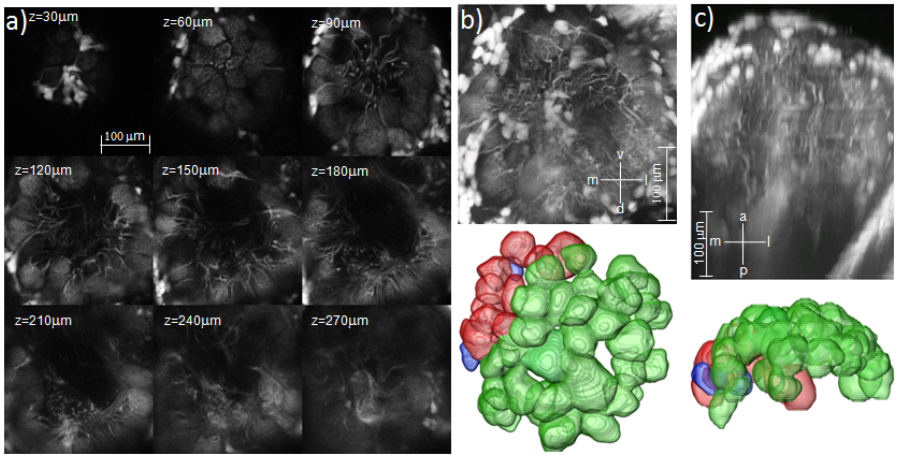

Fig. 6. – a) Image stack examples down to 270μm penetration depth into the right AL. b) Projection view along the anterior-posterior axis (above) and reconstructed glomerular volume images (below). c) Projection view along the dorso-ventral axis (above) and reconstructed glomerular volume images (below). Glomeruli coloured in green are from the T1 region projecting into the l-ACT, the blue glomeruli are from the T2 region, red ones from the T3 region, the last two projecting into the m-ACT.

time we were able to optically record activity also from these glomeruli deep within the antennal lobe.

The response of the surface glomeruli was compared to experiments using wide field fluorescence [12, 23]. In most of the cases the normalized response signals agree to the reported values or are found to be slightly higher, which might be explained by the higher sensitivity of our imaging system. The main responses to 1-Hexanol are coming from glomeruli T1-28, T1-36, and T1-52. Among the T1-glomeruli imaged for the first time, the most strongly responding glomeruli are T1-20 and T1-34. Glomerulus T1-23 shows a strong inhibitive response. The T3 glomeruli, most of them imaged for the first time, show mainly responses of medium strength and duration. The first image of a glomerulus of the T2 class (T2-1(2)) shows as a characteristic an extremely long response delay, which confirms electrophysiological studies [19, 20].

These data demonstrate that we created optical access to the profound glomeruli of the T2 and T3 classes projecting into the m-ACT and thus made straight path to the exploration of a whole new branch of the olfactory processing network, which so far could be investigated only partially by electrophysiological methods [19, 20] or at the level of the axon terminals [21]. Strong activity signals and high temporal resolution are also here giving hope to a much needed systematical expansion of the odour response maps including these new glomerular classes.

4. – Conclusion

The functional data acquired by two-photon microscopy we have presented in this work suggest that our imaging platform offers the capability to extend the specific AL odour response maps which have been measured in the past for many different odour components and in most of the T1 glomeruli [12]. So far these maps contain only the static

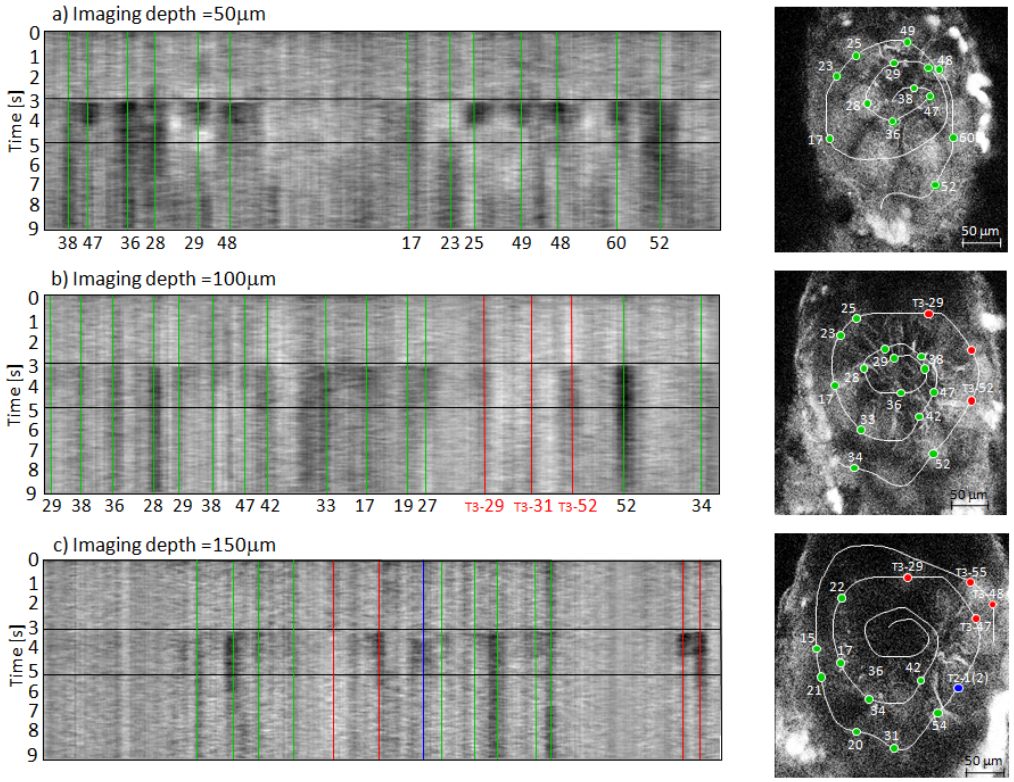

Fig. 7. – Odor response maps of a left AL to 1-Hexanol stimuli recorded at different imaging depth: 50μm in (a), 100μm in (b), and 150μm in (c). The Calcium response maps are shown together with the imaging planes and the corresponding laser scan traces. The responding centres are labelled by the corresponding glomerular number. T1 glomeruli are labelled by numbers only, the others by the sensor tract T2,T3, respectively, and the corresponding number.

parameters response strength and consistency range, which might now be supplemented by adding temporal features as the response latency or oscillatory components. The intrinsic axial resolution and the extended imaging depth of two-photon microscopy has allowed us to resolve profound functional data. Odor response maps could therefore be completed by measuring glomeruli of the more profound classes T2,T3, and T4.

This new possibility is of special interest because these glomerular classes are projecting into the m-ACT axonal tract and have been hypothesized to show fundamental differences regarding their odour coding properties [19, 20, 21], as well as their memory related plasticity after odour conditioning [23]. The morphological division of the olfactory pathway into the two axonal tracts [10] seems to be accompanied by a functional division into two parallel processing branches. We have now for the first time created optical access to the m-ACT branch in the antennal lobe which allows for a systematic study of the complete odour code.

In addition we have obtained a 4-fold increase in the functional-related fluorescence change with respect to similar experiments using wide field imaging. Another promising feature of the two-photon microscopy approach is the possibility to investigate sub-

glomerular structures down to single neurons [8]. This becomes even more crucial if imaging is extended to higher order brain centres such as the mushroom body, where a meta-structure comparable to the AL's glomeruli is absent [26]. Finally, aside the resolution's improvements, the intrinsic two-photon limited photo-damage has offered extended imaging sessions up to 5 hours. This should allow in the future for in-vivo real time studies of the antennal lobe plasticity after odour conditioning [16].

* * *

We wish to thank T. Franke, J. Rybak, and R. Menzel for helpful discussions. The project was funded by the Provincia Autonoma di Trento (project COMNFI).

REFERENCES

[1] Hodgkin A. L. and Huxley A. F., *Nature*, **144** (1939) 710.
[2] Salzberg B. M., Cohen L. B., and Davila H. V., *Nature*, **246** (1973) 508.
[3] Grynkiewicz G., Poenie M., and Tsien R. Y., *J. Biol. Chem.*, **260** (1985) 3440.
[4] Denk W., Strickler J., and Webb W., *Science*, **248** (1990) 73.
[5] Svoboda K., Denk W., Kleinfeld D., and Tank D. W., *Nature*, **385** (1997) 161.
[6] Menzel R. and Giurfa M., *Trends Cognit. Sci.*, **5** (2001) 62.
[7] Brandt R., Rohlfing T., Rybak J., Krofczik S., Maye A., Westerhoff M., Hege H.-C, and Menzel R., *J. Comp. Neurol.*, **492** (2005) 1.
[8] Franke T., *In vivo 2-photon calcium imaging of olfactory interneurons in the honeybee antennal lobe*, Dissertation, (FB Biologie, Chemie, Pharmazie, Freie Universität Berlin) 2009.
[9] Flanagan D. and Mercer A. R., *Int. J. Insect Morphol. Embryol.*, **18** (1989) 145.
[10] Kirschner S., Kleineidam C. J., Zube C., Rybak J., Grünewald B., Rössler W., *J. Comp. Neurol.*, **499** (2006) 933.
[11] Lieke E. E., *Eur. J. Neurosci.*, **5** (1993) 49.
[12] Galizia C.G., Sachse S., Rappert A.,and Menzel R., *Nat. Neurosci.*, **2** (1999) 473.
[13] Gelperin A. and Flores J., *J. Neurosci. Meth.*, **72** (1997) 97.
[14] Sachse S. and Galizia C. G., *J. Neurophysiol.*, **87** (2002) 1106.
[15] Galizia C. G., McIlwrath S. L., and Menzel R., *Cell Tissue Res.*, **295** (1999) 383.
[16] Hourcade B., Perisse E., Devaud J.M., and Sandoz J. C., *Learn. Mem.*, **16** (2009) 607.
[17] Galizia C. G. and Menzel R., *J. Insect Physiol.*, **47** (2001) 115.
[18] Moreaux L. and Laurent G., *Front. Neural Circuits*, **1** (2007) 2.
[19] Müller D., Abel R., Brandt R., Zöckler M., and Menzel R., *J. Comp. Physiol. A*, **188** (2002) 359.
[20] Krofczik S., Menzel R. and Nawrot M. P., *Front Comput Neurosci.*, **2** (2008) 9.
[21] Yamagata N., Schmuker N., Szyszka P., Mizunami M., and Menzel R., *Front. Syst. Neurosci.*, **3** (2009) 16.
[22] Galizia C. G. and Vetter R., *Optical methods for analyzing odor-evoked activity in the insect brain*, in *Advances in Insect Sensory Neuroscience*, edited by Christensen T. A. (CRC press, Boca Raton) 2004, pp. 349-392.
[23] Peele P., Ditzen M., Menzel R., and Galizia C. G., *J. Comp. Physiol. A*, **192** (2006) 1083.
[24] Sachse S.,Rappert A. and Galizia C. G., *Eur. J. Neurosci.*, **11** (1999) 3970.
[25] Laurent G., *Nat. Rev: Neurosci.*, **3** (2002) 884.
[26] Faber T. and Menzel R. , *Naturwissenschaften*, **88** (2001) 472.